COBEM UBERLÂNDIA 2019

ABCM Associação Brasileira de Engenharia e Ciências Mecânicas

25th ABCM International Congress of Mechanical Engineering
October 20-25, 2019, Uberlândia, MG, Brazil

COB-2019-2425
THE INFLUENCE OF AGING ON NI-RICH NI-TI PSEUDOELASTIC SPRINGS

Hugo de Souza Oliveira
Federal University of Bahia
oliveira.hugo@ufba.br
Aline Souza de Paula
University of Brazilia
alinedepaula@unb.br

Abstract. *The influence of heat treatments on Ni(50.7%)-Ti springs is analyzed regarding the hysteresis loop area, distribution of precipitates in the microstructure, and transformation temperatures. Solubilization followed by aging at 300°C, 400°C, and 500°C are performed in order to precipitate Ni_3Ti_4 particles. Then the springs are cycled following a loading path seeking to stabilize its hysteretic response. It was found that intermediate aging temperatures produces higher hysteresis loop areas when compared to low aging temperatures. Results also showed how these areas change with temperature variation.*

Keywords: *Pseudoelasticity, Hysteresis Loop, Energy Dissipation, Precipitates*

1. INTRODUCTION

Shape memory alloys consist of a unique class of shape memory material that presents the ability to respond to external *stimuli*, such as heat, force, and magnetism (Duerig *et al.*, 1990; Otsuka and Ren, 2005; Lagoudas, 2008; Mahmud, 2009). Among the many existing shape memory alloys, the binary NiTi alloy has been one of the most studied for its shape memory effect and the pseudoelasticity phenomena, in addition to its intense nonlinear response under certain conditions (Otsuka and Ren, 2005; Lagoudas, 2008).

Regarding the material aspects of the NiTi alloys, a large amount of data is available in the literature. One of the most exciting discussions has been devoted to the multistage martensitic transformations and their causes (Khalil-Allafi *et al.*, 2002; Fan *et al.*, 2004; Zhou *et al.*, 2005; Fan *et al.*, 2006; Wang *et al.*, 2016). In addition to explaining the transformation sequences and the nature of the transformation peaks, these studies have been helpful in understanding the appearance of precipitates and how nickel concentration can vary in the microstructure of a Ni-rich NiTi alloy after heat treatment.

Concerning the ability to generate precipitates during aging, Ni-Ti alloys can be classified as follows: near-equiatomic (nickel concentration equal or below 50.5% Ni); and Ni-rich (nickel concentration above 50.5% Ni). Corresponding to these two classes, there are two main types of treatments: cold work with subsequent annealing, and aging, respectively. Even though many studies deal with the effect of heat treatment on pseudoelastic behavior and shape memory effect (Nishida *et al.*, 1986; Okamoto *et al.*, 1988; Duerig *et al.*, 1990; Lin and Wu, 1993; Liu and McCormick, 1994; Otsuka and Ren, 2005; Lagoudas, 2008), few papers have concentrated on the influence of heat treatments in the area and energy dissipation of the hysteresis loop.

This study addresses an analysis on how the hysteresis loop of Ni-rich NiTi springs are influenced by heat treatments and how the hysteresis loop area changes with temperature variation. It is important to understand the influence in the area once it can be crucial in dynamical applications involving the exploitation of pseudoelastic behavior.

2. HEAT TREATMENTS

2.1 Experimental procedures

We use 12 Ti-50.7% at Ni alloy springs from Kellogg's Research Labs with $N = 16$ windings, $c = 1mm$ wire radius and $r_0 = 9.7mm$ helix radius in order to study the influence of heat treatments. Initially, the heat treatments performed in NiTi springs are solubilization and ageing. Firstly, all springs are solubilized at 700°C for 1h to eliminate any dislocation and precipitates in the microstructure resulting from its manufacturing. Later, the springs are aged at 300°C, 400°C and 500°C for different time periods: 30min, 60min, 90min and 120min. Table 1 identifies each one of the 12 springs according to the ageing treatment.

Table 1: Aging performed after solubilization at 700°C without atmosphere protection

Time / Temperature	30min	60min	90min	120min
300°C	A1	A2	A3	A4
400°C	B1	B2	B3	B4
500°C	C1	C2	C3	C4

The works developed by Zhou *et al.* (2005),Wang *et al.* (2014), and Wang *et al.* (2016) reveal that ageing temperatures can be classified in terms of the effect they generate in the NiTi microstructure, such as (a)low temperatures (250°C–300°C); (b) intermediate temperatures (400°C–500°C); and (c) high temperatures(above 670°C–solubilization). Thus, this paper considers one low temperature and two intermediate temperatures. High temperatures are not considered in this investigation for they are very close to the solubilization temperature, where Ti_3Ni_4 are solubilized in the parent phase.

After each heat treatment, the springs are characterized through a DSC analysis using a Netzsch DSC 200 F3 equipment to identify the peak transformations and the corresponding temperatures. The temperature sweep is carried out at 10°C/min from 80°C to -60°C, identifying the direct transformations and from -60°C to 80°C, the reverse transformations.

2.2 Solubilization at 700°C

Figure 1 presents the transformations obtained after the solubilization at 700°C without atmosphere protection followed by quenching at 25°C. The main characteristic observed is the presence of only one peak in the direct and reverse transformation. According to Otsuka and Wayman (1999), Frick *et al.* (2005), and Fan *et al.* (2017), annealing causes the solution of exceeding Nickel. As a result, the microstructure does not present any precipitates. Therefore, the peak in the direct transformation represents a $B2 \rightarrow B19'$ (abbreviated as M) transition and the peak in the reverse transformation is the transition $B19' \rightarrow B2$.

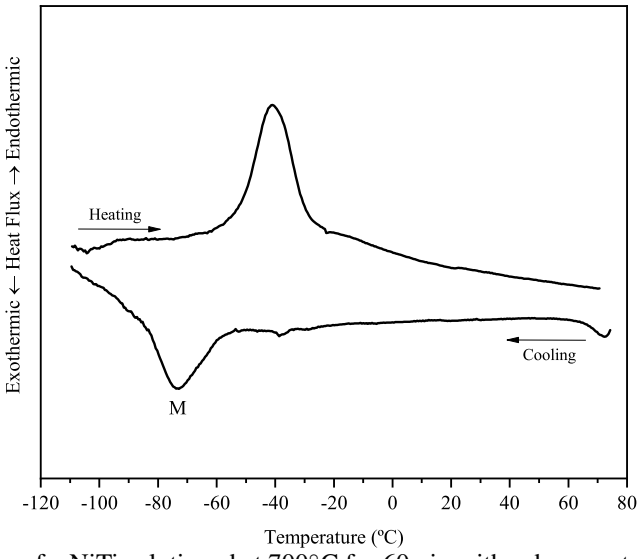

Figure 1: DSC curve of a NiTi solutioned at 700°C for 60min with subsequent quenching at 25°C.

Since no atmosphere protection was used, oxidation points such as Ti_4NiO_2, TiO_2 and TiC may be present in the microstructure. However, the time spent heat treating the springs is below the necessary for the oxidation points to penetrate the microstructure deeply (Mahmud, 2009). Accordingly, the influence of these points is inexpressive in this context.

2.3 Ageing at low and intermediate temperatures

While the transformation after solution treatment presents only one peak in DSC curves, representing one transformation, aged $NiTi$ alloys normally present two transformation stages $B2 \rightarrow R \rightarrow B19'$ and, consequently, two corresponding peaks (Zhou *et al.*, 2005).

The appearance of R phase prior to $B19'$ derives from the existence of Ni_4Ti_3 precipitates, formed while ageing

occurs (Wang *et al.*, 2016). These precipitates represent a strong resistance to the formation of $B19'$, which is associated with a larger deformation of the parent phase. In contrast, the R phase requires a smaller deformation and is much less influenced by the Ti_4Ni_3 particles (Zhou *et al.*, 2005).

2.3.1 Analysis of the transformations at 300°C

Figure 2(a) presents the DSC analysis of the 300°C aged spring (low temperature). In all cases, three transformation peaks can be found in the direct transformation. In similar experiments carried out by Zhou *et al.* (2005) and Wang *et al.* (2016), these peaks are related to two R transformations $B2 \rightarrow R1$ and $B2 \rightarrow R2$ with one transformation $R1 + R2 \rightarrow B19'$. Transformations $R1$ and $R2$ occur in different regions inside the grain

During ageing, as the nucleating barrier is much reduced at grain boundaries, the nucleation rate is higher (Zhou *et al.*, 2005). Therefore, the nucleation occurs more easily in this region when compared to the grain interior.

With the continuous precipitation of Ni_4Ti_3, Ni depletion at the grain boundaries is higher than in the interior. As the ageing temperature is low, Ni diffusion from the interior to the boundaries is much reduced and then Ni_4Ti_3 are formed in the grain interior as well due to the driving force of supersaturated Ni in the matrix (Zhou *et al.*, 2005; Wang *et al.*, 2016).

Figure 2(b) is based on the work developed by Zhou *et al.* (2005), and Wang *et al.* (2016). It schematically shows the microstructure obtained from a low temperature ageing. We can find a high concentration of precipitates in the grain interior along with a low concentration of Ni at the boundaries.

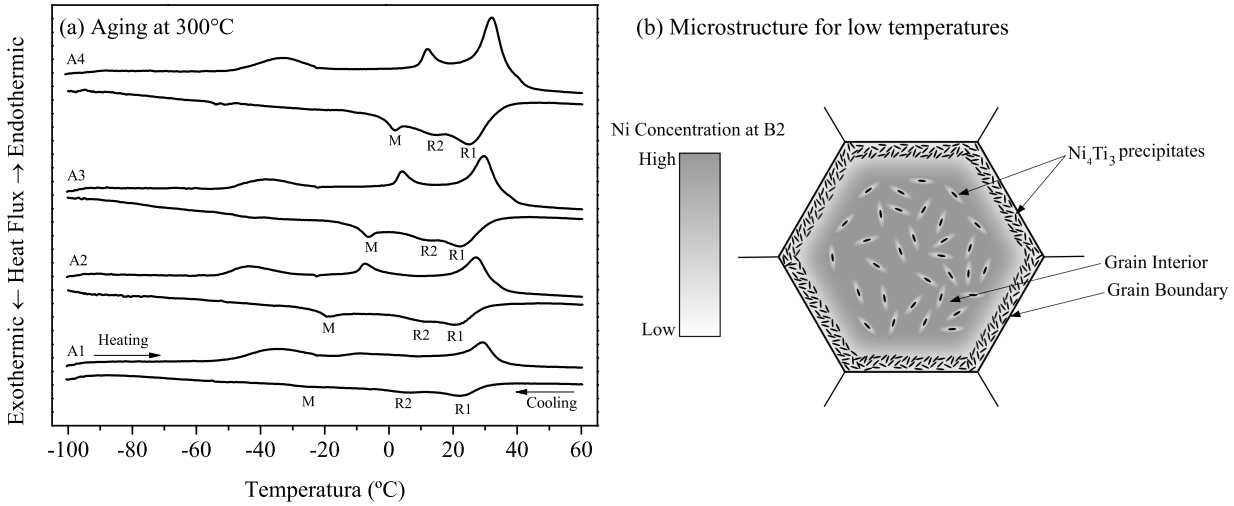

Figure 2: (a)DSC curves of a Ti-50.7% at Ni aged at 30min(A1), 60min(A2),90min(A3), and 120min(A4); (b)Schematic of the microstrucuture after ageing at 300°C.

The R-phase formation depends essentially on the Ni concentration and the strain field. Ni depletion affects the R-phase transformation temperature and the strain field favors the formation of R-phase thermodynamically (Wang *et al.*, 2016). In this sense, long precipitates produces a low distortion of the matrix and a higher Ni depletion, while small precipitates produces high distortion and shorter depletion.

Accordingly, the first peak in the direct transformation corresponds to the R phase transition at the grain boundaries $B2 \rightarrow R1$ (abbreviated as $R1$). With the continuous cooling, the grain interior experiences another R phase transition $B2 \rightarrow R2$ (abbreviated as $R2$), which is the second transformation peak (Wang *et al.*, 2014, 2015).

The third transformation peak is associated with the transition $R1 + R2 \rightarrow B19'$, i.e, the two R phases transform into the $B19'$ phase. In a similar analysis, Zhou *et al.* (2005) states that if only the Ni concentration heterogeneity is considered, the martensitic transformation would also occur in two steps — a transformation in the grain boundaries followed by another at the grain interior. However, $B19'$ transformations do not only depend on the Ni concentration, but also on the precipitates density. Thus, the lattice distortion resulting from the precipitates hampers the $B19'$ formation.

As a result, this transition becomes more difficult at the grain boundaries than in grain interior. Therefore, it is possible to observe that the heterogeneity distribution of precipitates acts as a contrary effect against the large-scale heterogeneity. Thus, these effects tend to cancel each other out, resulting in only one transformation stage $R1 + R2 \rightarrow B19'$ (Zhou *et al.*, 2005).

2.3.2 Analysis of the transformations at 400°C and 500°C

Figure 3 and 3(b) present the transformation peaks at 400°C and 500°C, respectively. Likewise the results obtained at 300°C, there are three transformation peaks. It is also possible to notice that as the ageing time increases, the peaks in

reverse transformation approach an overlapping tendency similarly to the results in Fan *et al.* (2004).

The overlapping tendency observed in 3(a) is consolidated in 3(b), where the first peak of the 30min and 60min aged reverse transformation represents the overlap of two peaks and the third peak is indicated by an arrow. The 90min and 120min aged cases have only one peak, representing the overlapping of three peaks.

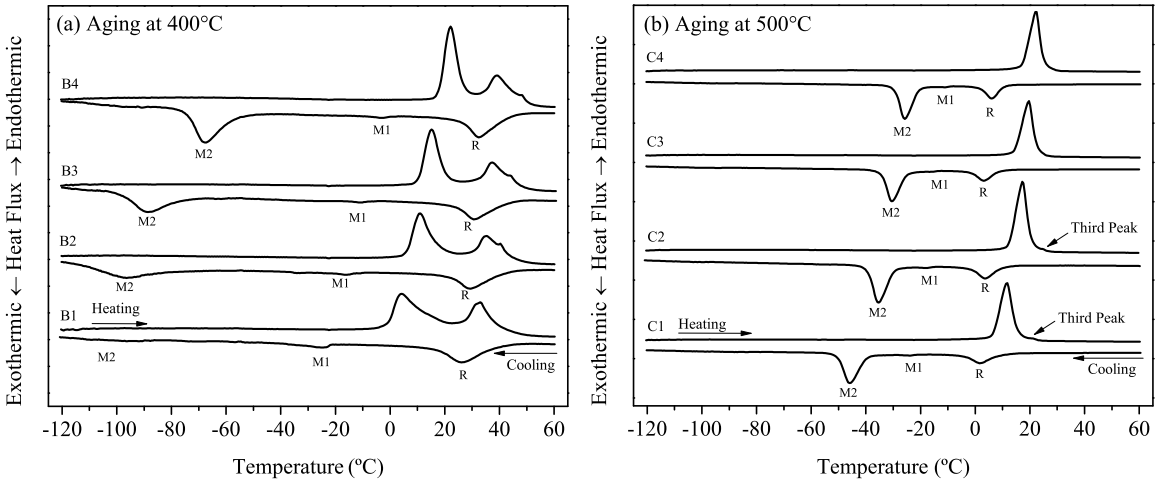

(c) Microstructure for high temperatures

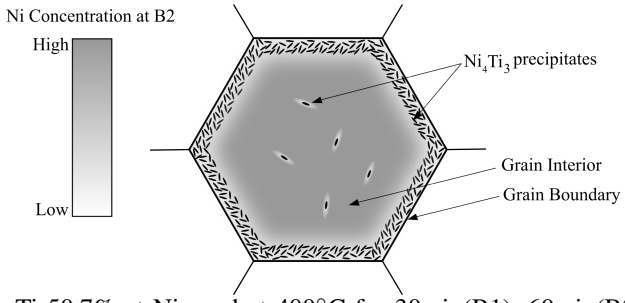

Figure 3: (a)DSC curves of a Ti-50.7% at Ni aged at 400°C for 30min(B1), 60min(B2),90min(B3), and 120min(B4); (b)DSC curves of a Ti-50.7% at Ni aged at 400°C for 30min(C1), 60min(C2),90min(C3), and 120min(C4);(c)Schematic of the microstrucuture after ageing at intermediate temperatures.

Similarly to what occurs at low-temperature ageing treatment, ageing at 400°C and 500°C also produces precipitates at the grain boundaries. However, the main difference lies in the grain interior. Low-temperature ageing results at a higher precipitation density in the grain interior due to the large-scale heterogeneity, while at intermediate temperatures the precipitation is lower because of the Ni diffusion from the interior towards the grain boundaries during ageing, resulting in a low Ni_4Ti_3 density in the grain interior Fan *et al.* (2004); Zhou *et al.* (2005); Wang *et al.* (2016).

According to Fan *et al.* (2004), the tension field at the grain boundaries reduces the nucleating driving force necessary to form Ni_4Ti_3. Such precipitation reduces the Ni concentration at $B2$ around them, favoring the transition $B2 \rightarrow R$ at the grain boundary.

The precipitates also favor the $B2 \rightarrow R$ when it imposes a resistance to the deformations related to the martensitic transformation $B2 \rightarrow B19'$ at the grain boundaries. Therefore, the first peak must be understood as $B2 \rightarrow R$ (abbreviated as R) at the grain boundaries.

The second transformation peak results from the transformation $B2 \rightarrow B19'$ (abbreviated as $M1$) at the grain interior. Differently from the cases at low temperatures, Ni migrates from the interior to grain boundaries, resulting in a lower Ni concentration, not favoring the formation of precipitate.

Regarding the third peak, it represents the transition $R \rightarrow B19'$ (abbreviated as M2). It occurs at temperature below M1 since the driving force is higher in this case, requiring low temperatures.

Figure 3(c) schematically illustrates the microstructure. It is possible to notice a high density of Ni_4Ti_3 at the grain boundaries and a low density in the interior. The Ni concentration difference between grain interior and boundary is also lower than in the case of low temperatures.

3. HYSTERESIS LOOP AND ENERGY DISSIPATION PER CYCLE

After heat treatments and DSC analysis, the influence of the microstructure in the hysteresis loop is analyzed. For this purpose, the hysteresis loop stabilization is performed at a constant temperature above A_f following a constant thermomechanical loading path. The springs are loaded over 50 cycle with a maximum load of 15N applied at 0.025N/s at a constant temperature.

According to Miyazaki *et al.* (1986) and Lagoudas (2008), stabilization is necessary for causing inelastic strains to saturate and introducing microstructural changes that result in macroscopically residual deformations. It is performed by means of a spring traction-machine specifically designed in Oliveira (2018) and built in the GDS(Group of Dynamical Systems) at the University of Brasilia.

After stabilization, the springs are loaded with 15N at a constant temperature defined as FTT (First Test Temperature). The FTT temperature is always above A_f and represents a point not influenced by any transformation of the last peak on the reverse transformation, that is, it may be different depending on the aging treatment and the last peak. This temperature is obtained from a visual observation of each DSC graph. Figure 4 presents a schematic illustration of the FTT point.

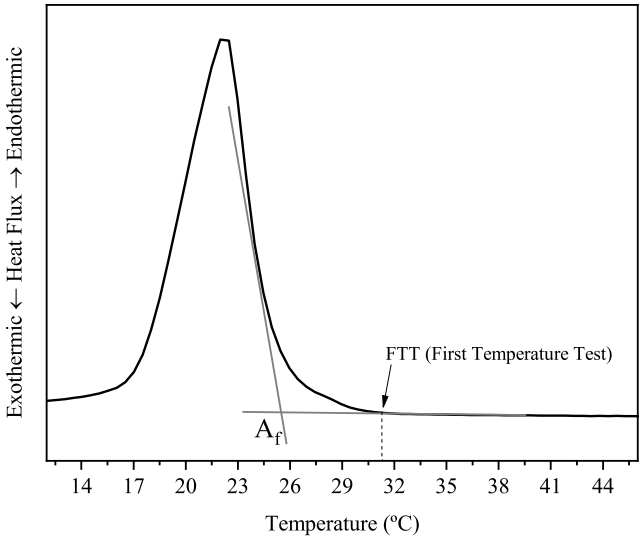

Figure 4: Schematic illustration of the FTT point definition.

3.1 Constant maximum load test

Figure 5(a) presents the 300°C aged springs hysteresis loops. Aging at this temperatures results in small areas. It is visible that the increase in ageing time does not produce any significant variations in the hysteresis loop area.

The DSC curves presented in Figure 2(b), reveal that heat treatments that result in high precipitates density both at the grain interior and boundaries generate small hysteresis loops areas and, consequently, low energy dissipation per cycle.

Figures 5(b) and 5(c) show the results for 400°C and 500°C ageing temperatures, respectively. When compared to 300°C aged springs, it is possible to observe that the microstructure associated with a low density of Ni_4Ti_3 in the grain interior combined with a high density at the boundaries results in larger hysteresis loops areas and higher energy dissipation per cycle.

Figure 6 reveals that ageing time is an important factor in the increase of the hysteresis area for intermediate temperatures. For example, a comparison of the 400ºC and 500ºC aged springs hysteresis areas indicates a difference that can reach up to 30% — for a 120-minute ageing — and 60% — for a 30-minute ageing.

The expressive increase in the hysteresis loop area of the springs aged at 400°C and 500°C in relation to those at 300°C can be explained through the microstructure characteristics. Aging at intermediate temperatures generates high precipitation density at the grain boundaries, while its interior remains free or with a very low precipitate density. Therefore, this microstructure associates with a high dissipation of energy per cycle, when compared to the hysteresis loop obtained at low temperatures.

3.2 Hysteresis loop area change due to temperature variation

In order to exploit the pseudoelasticity in dynamical systems, the test temperature must be always above A_f. However, the hysteresis loop area can be altered even when in a pseudoelastic regime by increasing the test temperature.

Figure 7(a) presents the influence of the temperature increase in the hysteresis loop area above A_f. In this analysis, increments of 1°C were considered starting at the FTT temperature of each spring. The results demonstrate how the area

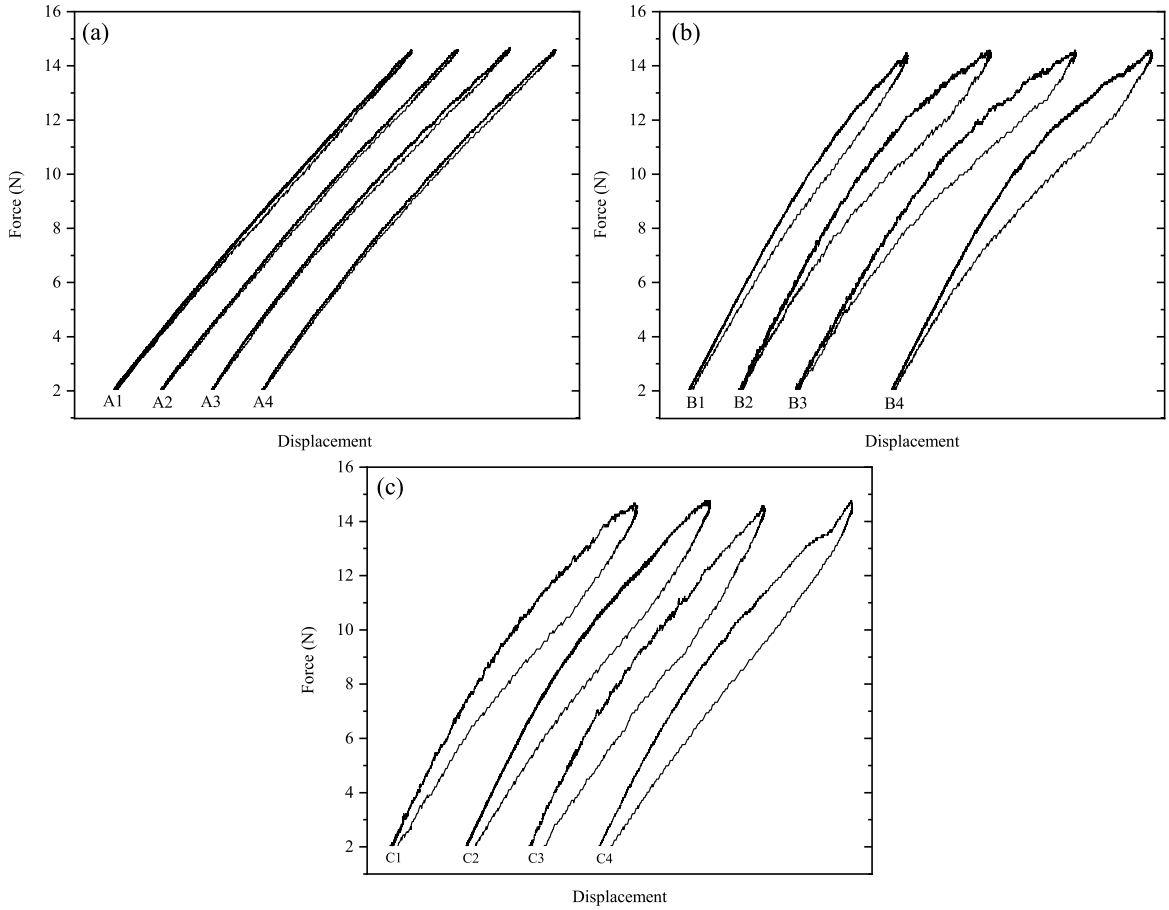

Figure 5: 15N loading applied at the FFT temperature of each spring. (a) Springs aged at 300ºC: A1=35°C; A2=47°C; A3=47°C; A4=48°C. (b) springs aged at 400ºC: B1=54°C; B2=54°C; B3=56°C; B4=55°C. (c)springs aged at 500ºC: C1=34°C; C2=34°C; C3=36°C; C4=55°C.

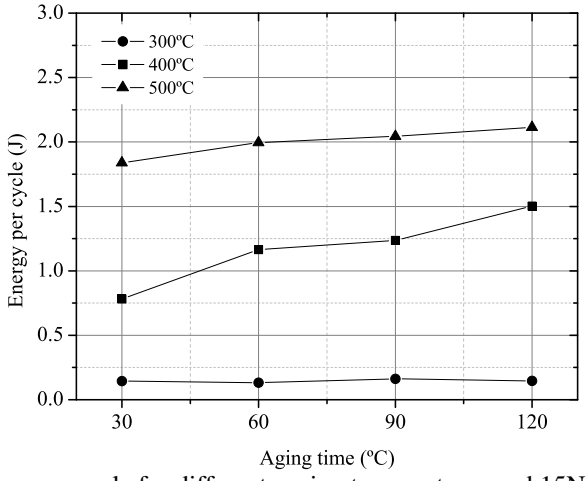

Figure 6: Energy dissipation per cycle for different ageing temperatures and 15N maximum constant load.

can be reduced by means of the temperature increase for each spring. Figure 7(b) presents the energy dissipation cycle rate reduction for each spring.

As presented in 7(a), for the 500ºC aged springs, higher test temperatures are associated with smaller hysteresis loop area. However, the reduction rate of the dissipated energy per cycle, shown in 7(b), increases with the ageing time. For the 400ºC aged springs, it is possible to observe higher reduction rate with ageing time from 30min to 90min. This rate softly decreases from 90min to 120min.

The 300ºC aged springs present a very low hysteresis area, as presented in Figure 9. Figure 10 illustrates that the area reduction rate does not present significant variation.

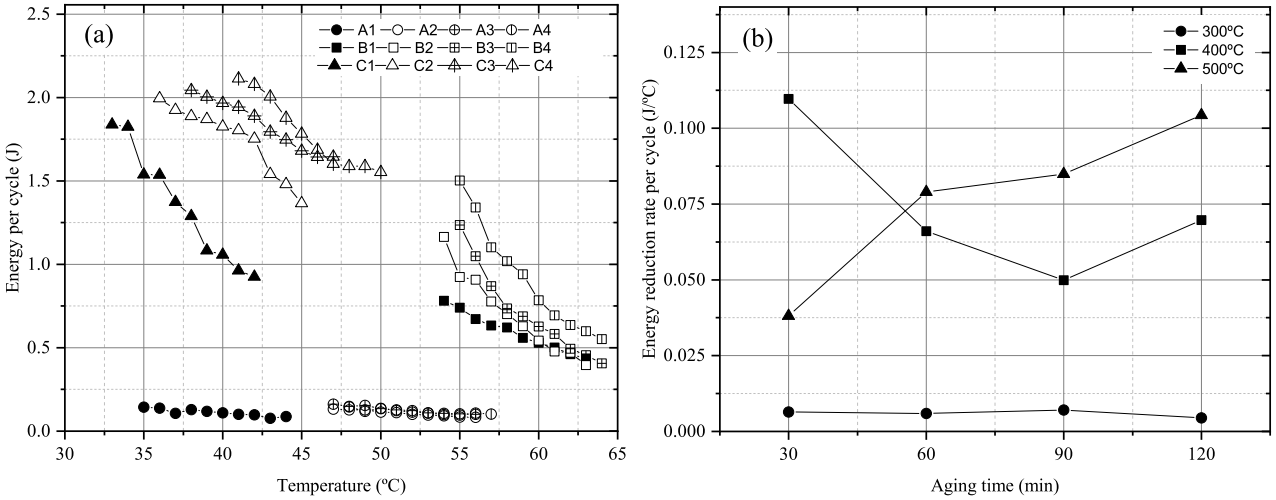

Figure 7: (a)Energy dissipation variation with test temperature; (b)Energy dissipation per cycle rate reduction.

4. CONCLUSION

Our contribution encompasses the analysis of the influence of heat treatments on the hysteresis loop area of a Ni-rich NiTi spring. In all heat treatments performed, the results are in agreement with the literature, especially the transformation peaks that allowed to describe the material microstructure. The 300ºC aged springs are described as having a high concentration of precipitates in the grain interior along with a low concentration of Ni at the boundaries. The 400ºC and 500ºC aged springs are described as having a high density of Ni_4Ti_3 at the grain boundaries and a low density in the interior.

The *quasi*-static tests revealed that intermediate aging temperatures (400°C–500°C) produce higher hysteresis areas in relation to those performed at low aging temperatures (250°C–300°C). It also revealed how the hysteresis loop area changes with temperature increase. These results represent a contribution for further researches and technological developments in which the hysteresis loop area is significant, such as dynamical applications where the energy dissipation can be critical.

5. ACKNOWLEDGEMENTS

The authors would like to thank the Brazilian Research Agencies CNPq, CAPES,Mecanon Research Group, and, professor Marcelo Savi.

6. REFERENCES

Duerig, T.W., Melton, K.N., Stöckel, D. and Wayman, C.M., 1990. *Engineering Aspects of Shape Memory Alloys*. Elsevier. ISBN 978-0-7506-1009-4. doi:10.1016/C2013-0-04566-5. URL https://linkinghub.elsevier.com/retrieve/pii/C20130045665.

Fan, G., Chen, W., Yang, S., Zhu, J., Ren, X. and Otsuka, K., 2004. "Origin of abnormal multi-stage martensitic transformation behavior in aged Ni-rich Ti-Ni shape memory alloys". *Acta Materialia*, Vol. 52, No. 14, pp. 4351–4362. ISSN 1359-6454. doi:10.1016/j.actamat.2004.06.002.

Fan, G., Zhou, Y., Chen, W., Yang, S., Ren, X. and Otsuka, K., 2006. "Precipitation kinetics of Ti3ni4 in polycrystalline Ni-rich TiNi alloys and its relation to abnormal multi-stage transformation behavior". *Materials Science and Engineering: A*, Vol. 438-440, No. SPEC. ISS., pp. 622–626. ISSN 0921-5093. doi:10.1016/j.msea.2006.02.066. URL http://linkinghub.elsevier.com/retrieve/pii/S0921509306005636.

Fan, Q.C., Zhang, Y.H., Wang, Y.Y., Sun, M.Y., Meng, Y.T., Huang, S.K. and Wen, Y.H., 2017. "Influences of transformation behavior and precipitates on the deformation behavior of Ni-rich NiTi alloys". *Materials Science and Engineering: A*, Vol. 700, pp. 269–280. ISSN 0921-5093. doi:10.1016/j.msea.2017.05.107. URL http://www.sciencedirect.com/science/article/pii/S0921509317307384.

Frick, C.P., Ortega, A.M., Tyber, J., Maksound, A., Maier, H.J., Liu, Y. and Gall, K., 2005. "Thermal processing of polycrystalline NiTi shape memory alloys". *Materials Science and Engineering: A*, Vol. 405, No. 1-2, pp. 34–49. doi:10.1016/j.msea.2005.05.102. URL http://linkinghub.elsevier.com/retrieve/pii/S0921509305005563.

Khalil-Allafi, J., Dlouhy, A. and Eggeler, G., 2002. "Ni4ti3-precipitation during aging of NiTi shape memory alloys and its influence on martensitic phase transformations". *Acta Materialia*, Vol. 50, No. 17, pp. 4255–4274. ISSN 1359-6454. doi:10.1016/S1359-6454(02)00257-4. URL http://www.sciencedirect.com/science/article/pii/

S1359645402002574.

Lagoudas, D.C., 2008. *Shape Memory Alloys: Modeling and Engineering Applications*. Springer. ISBN 978-0-387-47685-8. Google-Books-ID: NgHpMRUW_sIC.

Lin, H.C. and Wu, S.K., 1993. "Determination of heat of transformation in a cold-rolled martensitic tini alloy". *Metall. Trans. A*, Vol. 24, No. 2, pp. 293–299. ISSN 0360-2133. doi:10.1007/BF02657316. URL http://link.springer.com/10.1007/BF02657316.

Liu, Y. and McCormick, P.G., 1994. "Thermodynamic analysis of the martensitic transformation in NiTi—I. Effect of heat treatment on transformation behaviour". *Acta Metall. Mater.*, Vol. 42, No. 7, pp. 2401–2406. ISSN 09567151. doi:10.1016/0956-7151(94)90318-2. URL http://linkinghub.elsevier.com/retrieve/pii/0956715194903182.

Mahmud, A.S., 2009. *Thermomechanical treatment of ni-ti shape memory alloy*. Phd thesis, The University of Western Australia, Perth, Australia.

Miyazaki, S., Imai, T., Igo, Y. and Otsuka, K., 1986. "Effect of cyclic deformation on the pseudoelasticity characteristics of Ti-Ni alloys". *Metallurgical Transactions A*, Vol. 17, No. 1, pp. 115–120. doi:10.1007/BF02644447. URL https://link.springer.com/article/10.1007/BF02644447.

Nishida, M., Wayman, C.M. and Honma, T., 1986. "Precipitation processes in near-equiatomic TiNi shape memory alloys". *Metall. Trans. A*, Vol. 17, No. 9, pp. 1505–1515. doi:10.1007/bf02650086.

Okamoto, Y., Hamanaka, H., Miura, F., Tamura, H. and Horikawa, H., 1988. "Reversible changes in yield stress and transformation temperature of a NiTi alloy by alternate heat treatments". *Scr. Metall.*, Vol. 22, No. 4, pp. 517–520. doi:10.1016/0036-9748(88)90016-6.

Oliveira, H.S., 2018. *Analise da influencia do tratamento termico deligas Niti em aplicacoes dinamicas*. Ph.D. thesis, Universidade de Brasilia.

Otsuka, K. and Ren, X., 2005. "Physical metallurgy of Ti–Ni-based shape memory alloys". *Progress in Materials Science*, Vol. 50, No. 5, pp. 511–678. ISSN 00796425. doi:10/fqvczb. URL http://linkinghub.elsevier.com/retrieve/pii/S0079642504000647.

Otsuka, K. and Wayman, C.M., 1999. *Shape Memory Materials*. Cambridge University Press. ISBN 978-0-521-66384-7. Google-Books-ID: DvItE9XUlN8C.

Wang, X., Kustov, S., Li, K., Schryvers, D., Verlinden, B. and Van Humbeeck, J., 2015. "Effect of nanoprecipitates on the transformation behavior and functional properties of a Ti–50.8at.% Ni alloy with micron-sized grains". *Acta Materialia*, Vol. 82, pp. 224–233. ISSN 1359-6454. doi:10.1016/j.actamat.2014.09.018. URL http://www.sciencedirect.com/science/article/pii/S1359645414006971.

Wang, X., Li, K., Schryvers, D., Verlinden, B. and Van Humbeeck, J., 2014. "R-phase transition and related mechanical properties controlled by low-temperature aging treatment in a Ti-50.8 at.% Ni thin wire". *Scripta Materialia*. ISSN 13596462. doi:10.1016/j.scriptamat.2013.10.006.

Wang, X., Verlinden, B. and Kustov, S., 2016. "Multi-stage martensitic transformation in Ni-rich NiTi shape memory alloys". *Functional Materials Letters*, Vol. 10, No. 01, p. 1740004. ISSN 1793-6047. doi:10.1142/S1793604717400045. URL https://www.worldscientific.com/doi/abs/10.1142/S1793604717400045.

Zhou, Y., Zhang, J., Fan, G., Ding, X., Sun, J., Ren, X. and Otsuka, K., 2005. "Origin of 2-stage R-phase transformation in low-temperature aged Ni-rich Ti–Ni alloys". *Acta Materialia*, Vol. 53, No. 20, pp. 5365–5377. ISSN 1359-6454. doi:10.1016/j.actamat.2005.08.013. URL http://www.sciencedirect.com/science/article/pii/S1359645405004751.

7. RESPONSIBILITY NOTICE

The author are the only responsible for the printed material included in this paper.